PROCEEDINGS OF SCIENCE

The scientific results from the X-ray observatory *Hitomi*

Manabu Ishida*
The Institute of Space and Astronautical Science / JAXA, Japan
E-mail: ishida@astro.isas.jaxa.jp

Hitomi is the 6th Japanese X-ray astronomy satellite launched on 2016 Feb 17. Although it was unfortunately lost about 1 month from the launch, *Hitomi* produced many new scientific results, owing to extremely high spectral resolution of the non-dispersive SXS detector (X-ray micro-calorimeter). From the observations of the Perseus cluster, a stringent upper limit of the turbulent pressure, only $<7\%$ of that of the thermal pressure, is obtained, and the metal abundance in ICM is found consistent to that of the solar vicinity. Power of the high resolution spectroscopy even with small photon counts is demonstrated in N132D and IGR J16318-4848. Emission/absorption line search was performed in Crab and G21.5−0.9. A result is obtained to support that the Crab nebula was born from an electron-capture supernova. New absorption line structures are detected from G21.5−0.9, although they need further confirmation because of low statistical significance of 3-4σ. To fulfill the calorimeter science, the *XRISM* project has been on-going. Following *XRISM*, we have started preparing the next generation hard X-ray mission *FORCE* that is a successor of the hard X-ray imager onboard *Hitomi*, but with much better spatial resolution of 15 arcsec in HPD. They are planned to be launched by the end of March 2022 and late 2020's, respectively.

Multifrequency Behaviour of High Energy Cosmic Sources - XIII - MULTIF2019
3-8 June 2019
Palermo, Italy

*Speaker.

PoS(MULTIF2019)041

1. Introduction to *Hitomi* observatory

Hitomi, originally named *ASTRO-H* prior to the launch, is the 6th Japanese X-ray astronomy satellite developed by JAXA, under vast international collaboration including NASA, ESA, CSA and so on [1]. Figure 1 shows a schematic view of allocation of the *Hitomi* scientific instruments. Two kinds of X-ray mirror assemblies, Soft X-ray Telescope (SXT:[2, 3]) and Hard X-ray Tele-

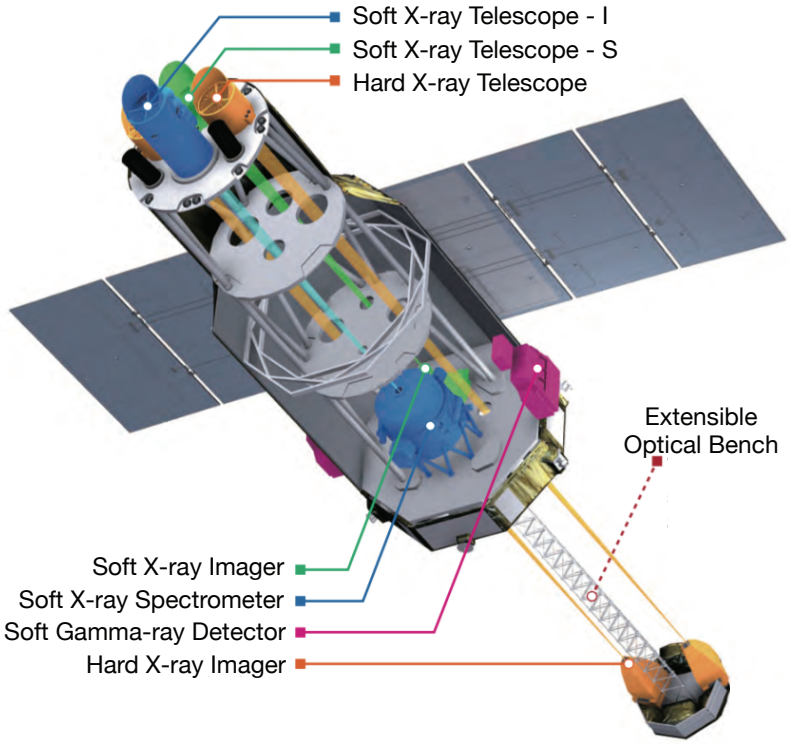

Figure 1: Overview of the *Hitomi* observatory

scope (HXT: [4, 5, 6]) are mounted on top of the optical bench. The SXT and HXT have equivalent two modules each. The SXTs have a focal length of 5.6 m, and on the focal plane of the SXT-S and SXT-I, the Soft X-ray Spectrometer (SXS: [7]) and the Soft X-ray Imager (SXI: [8]) are fabricated, respectively. On the other hand, the two Hard X-ray Imagers (HXIs: [9]) are mounted on the focal plane of the HXTs. Since the focal length of the HXTs is as long as 12 m, the HXIs are assembled on a separate plate connected at the end of the extensible optical bench (EOB), which is deployed after the launch. In addition to the detector systems with focusing optics described above, the Soft Gamma-ray Detectors (SGDs: [10]) are attached onto side panels of the spacecraft. The SGD also has two modules. All the detector systems are co-aligned so that they can observe the same target simultaneously.

In Fig. 2 we show the energy band that is covered with all the detector systems onboard *Hitomi*. *Hitomi* covers the band from 0.2 keV to 600 keV with moderate energy overlaps among the four detector systems.

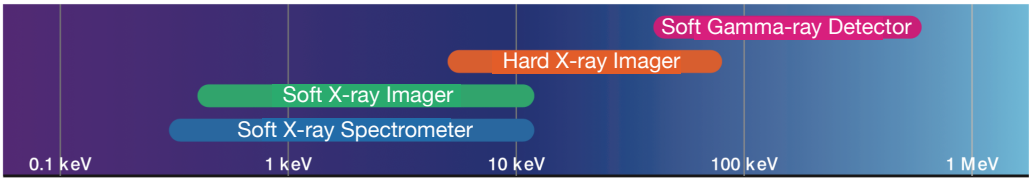

Figure 2: The energy band covered with the *Hitomi* detectors.

2. *Hitomi* observations and scientific results

2.1 Summary of the observations and the Soft X-ray Spectrometer (SXS)

In Fig. 3, we summarize the order of starting up the detector systems across the time line, together with targets in the field of view that is common among the detector systems. The commissioning of science instruments began with the SXS about one week after the launch 2015 February 17th, followed by the SXI, HXI, and SGD in this order. Unfortunately, *Hitomi* was lost on 2015 March 26th due to malfunction of the attitude & orbit control system, and was broken up into several pieces in its orbit. During one month from the commissioning start, we have data on six targets, as shown in Fig. 3.

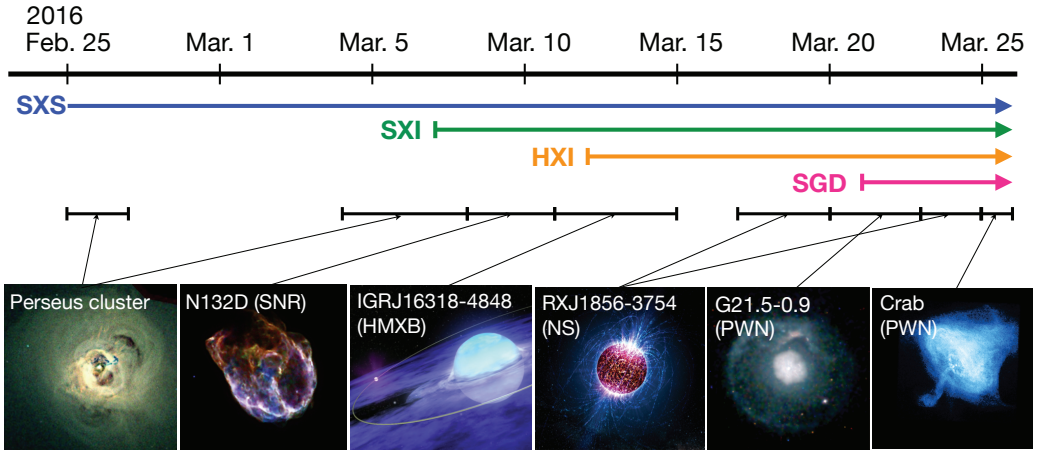

Figure 3: The energy band covered with the *Hitomi* detectors.

In this paper, we hereafter concentrate on scientific results obtained with the SXS. This is because the SXS is one of the main instruments of *Hitomi*, and it provides us with the highest spectral resolution data that have never been achieved in the X-ray band above 2 keV.

The Soft X-ray Spectrometer, or the SXS, is the X-ray micro-calorimeter which detects an X-ray photon as a slight increase of temperature of an X-ray absorber made of mercury telluride (HgTe). For this to be possible, the absorber is thermally connected to a heat sink which is cooled to a temperature of $\sim$50 mK. Since the heat capacity of a solid is proportional to T^3 in an extremely low-temperature environment, it becomes possible to detect tiny temperature increase caused by a single X-ray photon.

Figure 4 shows the effective area of the SXT-S/SXS system for a point source and the energy-resolving power of the SXS, compared with those of the grating systems onboard *Chandra* and

XMM-Newton. The effective are of the SXS is larger than the grating spectrometers of *Chandra* and *XMM-Newton* above 0.6 keV. The energy resolution, on the other hand, is better with the grating spectrometers in lower energy band. The SXS is more advantageous above 2 keV. In Fig. 5

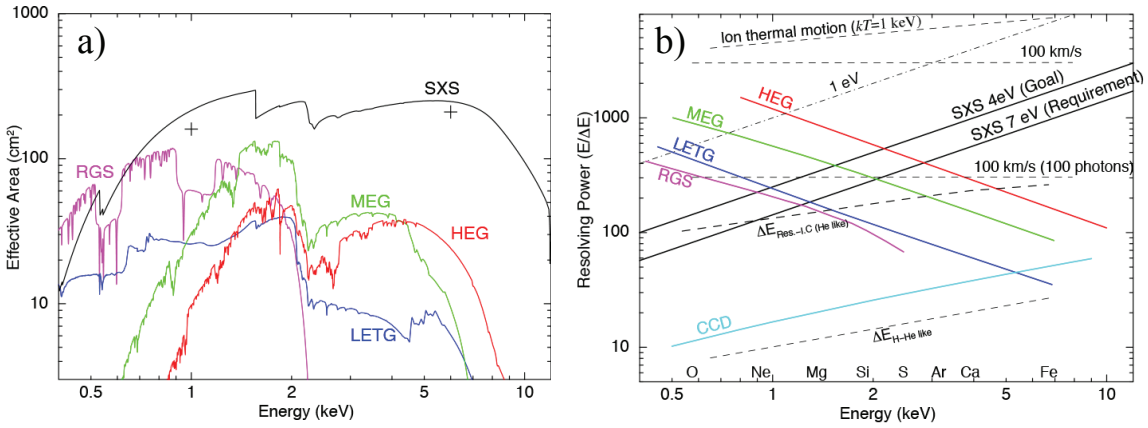

Figure 4: a) Effective area, and b) energy-resolving power of the micro-calorimeter SXS.

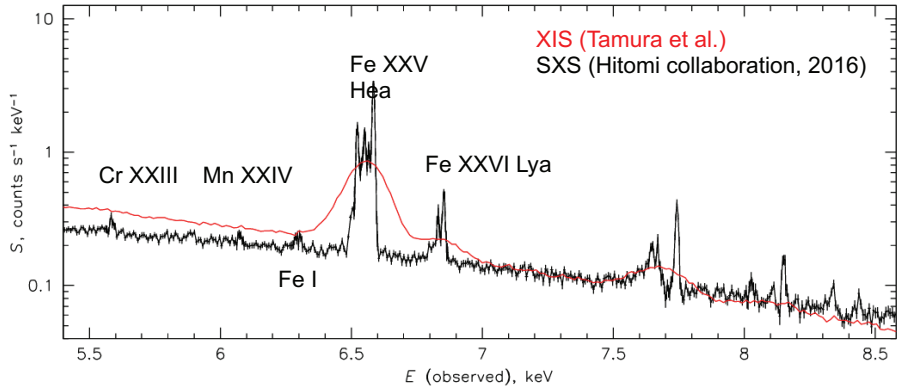

Figure 5: An X-ray spectrum of Perseus cluster taken with the SXS, together with that of the *Suzaku* CCD cameras for comparison ([11]).

we show an X-ray spectrum of the core of Perseus cluster taken with the SXS, together with that taken with the XIS (CCD camera) onboard *Suzaku* ([11]). A couple of humps at apparent energies of ∼6.6 keV and ∼6.8 keV correspond to K-shell emission lines from He-like and hydrogenic iron lines (so-called Heα and Lyα lines), respectively. A CCD camera, which is a standard imaging detector widely used by current X-ray missions, can only resolve emission lines of the same atomic species in different ionization states. The SXS, on the other hand, can resolve atomic transitions from different angular momentum states of the same ionization state. The spectral resolution at 5.9 keV is 4.97 eV in FWHM, which means the energy resolving power $E/\Delta E = 1250$. This is ∼30 times as powerful as that of the CCD cameras.

2.2 The Perseus cluster

The Perseus cluster is the X-ray-brightest nearby galaxy cluster with a redshift $z = 0.01756$.

The cluster is filled with a hot plasma with a temperature of 5×10^7 K. *Hitomi* observed this cluster for 290 ks in total. In this section we overview scientific results obtained from the Perseus cluster.

2.2.1 Measurements of dynamical motions

Hitomi examined motions of the hot gas within central 200 kpc region of the Perseus cluster [12, 13]. Figure 6 shows an SXS spectrum of the Perseus cluster averaged over the central ∼60 kpc region. A bulk velocity of the hot gas and its velocity dispersion are evaluated from centroids

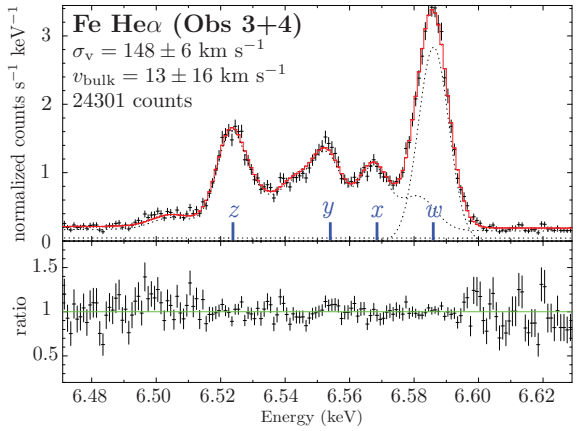

Figure 6: The SXS spectrum of the central 3×3 arcmin region of Perseus cluster [13].

and energy widths of these lines, respectively. In the central region, the hot gas does not show any significant bulk velocity (13±16 km s^{-1}) relative to the cD galaxy NGC 1275. Thanks to the high spectral resolution of the SXS, the velocity dispersion is successfully measured to be 148±6 km s^{-1} [13]. Figure 7 shows distributions of the bulk velocity and the velocity dispersion of the central 200 kpc region of the Perseus cluster [13]. In panel a), *Hitomi* detected a gradient of the

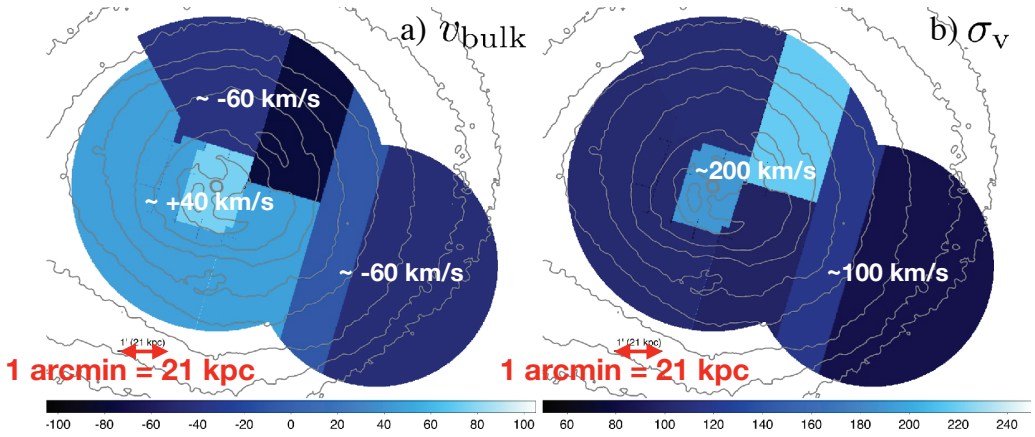

Figure 7: a) Bulk velocity and b) velocity dispersion of the central 200 kpc region of the Perseus cluster [13].

bulk velocity of 100 km s^{-1} across the cluster core. This can be interpreted as the sloshing motion by AGN [14] or a recent sub-cluster infall [15]. The velocity dispersion in panel b) is slightly

enhanced to 100-200 km s^{-1} at the center and the NW bubble, though it is less than 100 km s^{-1} in the other observed region. Gaussianity in the line profile indicates that the turbulence scale is less than 100 kpc. The ICM in the Perseus cluster is quiet and the dynamical support of the cluster relative to the thermal support $3\mu m_{\rm p}(v_{\rm bulk}^2+\sigma_v^2)/kT$ is only 0.02-0.07. This implies that we need not take into account the dynamical motion of the Perseus cluster hot gas in estimating the amount of dark matter.

2.2.2 Resonance scattering

It has been pointed out that the cluster hot gas can be optically thick for the resonance scattering. If so, the intensity of the resonance line is suppressed toward the cluster center whereas its intensity is enhanced in the cluster outskirts. In order to see if this is true, a detailed spectral analysis around the Heα line region of iron has been carried out. The SXS spectrum, together with the expected spectrum in red color, is shown in Fig. 8. It is confirmed that *w* component of the

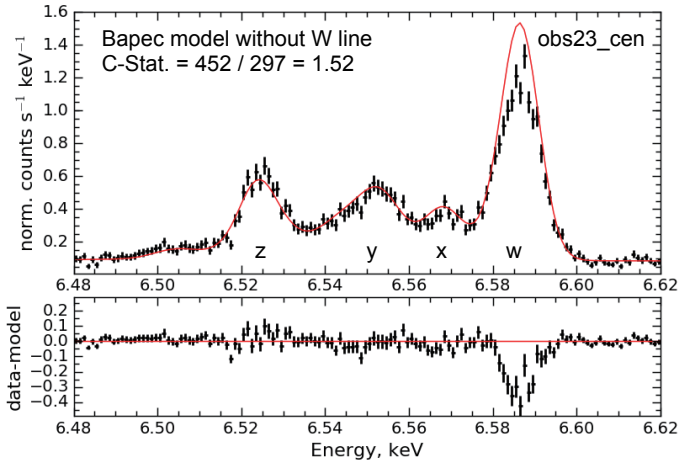

Figure 8: The SXS spectrum of Heα line region. The red curve shows the spectrum expected for the optically thin case [16].

iron Heα line is really suppressed in the central region of the Perseus cluster. A radial profile of *w*-component suppression out to 5′ ($\sim$100 kpc) indicates that its optical depth is $\tau = 2.27$ if $\sigma_{\rm v}$ = 0 km s^{-1}. Even if $\sigma_{\rm v}$ = 150-200 km s^{-1} [13], τ can be as large as unity. See [16] for more detail.

2.2.3 Measurements of temperatures

Prior to the advent of the high resolution spectrometers, such as the grating spectrometers onboard *Chandra* and *XMM-Newton*, plasma temperature of an X-ray-emitting hot plasma had been measured with a high-energy cutoff of a continuum spectrum. The high resolution spectrometers, now including the *Hitomi*'s SXS, enable us to measure plasma temperatures through intensity ratios of various lines. Since the SXS has better energy resolution above $\sim$2 keV (Fig. 4b), and larger effective area (Fig. 4a) than any other high resolution spectrometer, and is the only non-dispersive detector which is indispensable characteristic for diffuse X-ray sources, the SXS has been expected to surely make a breakthrough in the X-ray spectroscopy. The following kinds of the temperature can be measured through a spectroscopy with the SXS.

- Ionization temperature (T_Z) $\cdots$ can be measured with an intensity ratio of emission lines from different ionization states of the same element, such as Heα and Lyα of silicon, for example. This ratio depends upon an electron temperature T_e and the degree of ionization of the plasma. The latter can be parameterized with so-called the ionization parameter $n_e t$ where n_e is the electron density and t is the elapsed time since the onset of the plasma heating.

- Excitation temperature (T_e) $\cdots$ can be measured with an intensity ratio of emission lines from different excitation states of the same element in the same ionization state, such as Heα and Heβ (associated with the electron transition $n = 3 \rightarrow 1$), for example. This ratio depends only upon the electron temperature T_e.

- Ion temperature (T_{ion}) $\cdots$ is a kinetic temperature of an ion and can be measured through an energy width of any emission line.

In the case if the plasma is in complete thermal equilibrium, $T_Z = T_e = T_{ion}$ for all the elements. In the case of shock-heated ionizing plasma such as observed in SNR, $T_{ion} \gg T_e > T_Z$.

As an example, we show measurement of T_{ion} of the central region of the Perseus cluster in Fig. 9[17]. In this chart, the velocity dispersion —which is the σ of a Gaussian representing each

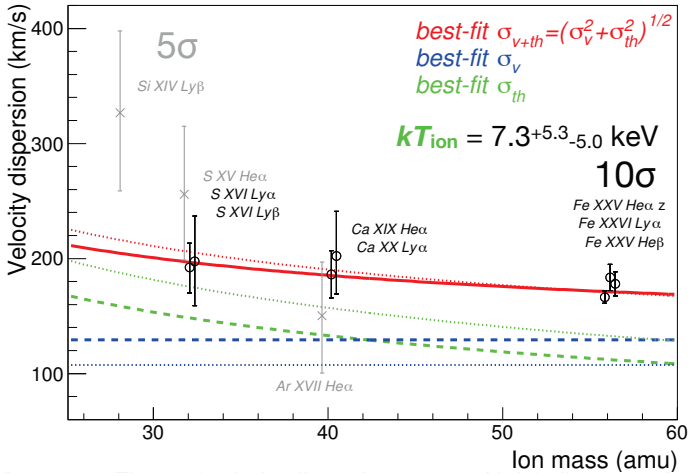

Figure 9: A chart of ion temperature measurement in the central region of the Perseus cluster[17].

emission line— of sulphur, calcium and iron in various ionization states are shown as a function of their atomic mass unit (amu). This is a root-mean-square of the width stemming from ion's thermal motion and that associated with the turbulent motion described in §2.2.1. Of them, the blue dashed line is the velocity dispersion of the turbulent motion, which is common among all the elements, and the green dashed curve is the line width associated with the ion's thermal motion. The red solid curve is the root-mean-square of them. The best-fit ion temperature is $T_{ion} = 7 \pm 5$ keV, which is consistent with the electron temperature. Note that we should utilize difference of the thermal velocities among different elements for measuring the ion temperature. For this to be done, it is understood from Fig. 9 that accurate measurements of the velocity dispersions of sulfur and calcium, in addition to those of iron, are indispensable. This is, however, hampered by the facts that the calcium lines are intrinsically very weak, and we have lost significant amount of the sulfur

photons, for lower energy X-rays were attenuated by the beryllium plate attached on the Dewar's gate valve, which had still been closed because *Hitomi* was still in the commissioning phase. The large errors of the velocity dispersions of sulfur and calcium result in the large error ($\pm$5 keV) on the ion temperature.

Since the cluster hot gas is formed through shock-heating of the cosmic primordial gas at around the virial radius, accelerated by the cluster's gravitational potential by the dark matter, the shocked ions should originally have much greater thermal energy than the electrons by their mass ratio. If such energy imbalance remains, the cluster should have a lot of "hidden" energy in the form of ions' dynamical motion. This could affect the estimation of the dark matter in the universe. The SXS measurement of $T_{\rm ion}$ is very important in that such possibility is denied at least for the central region of the Perseus cluster.

2.2.4 Metal abundance in ICM

Better energy resolution also contribute to enhance sensitivity to weak lines. As a matter of fact, as shown in Fig. 10, the SXS is able to unambiguously detect weak Kα emission lines from the rare metals, Cr and Mn (Fig. 10a), as well as to discriminate Heα triplet of Ni from Heβ of Fe (Fig. 10b). Note that the equivalent widths of Cr-Kα and Mn-Kα lines are only a few eV.

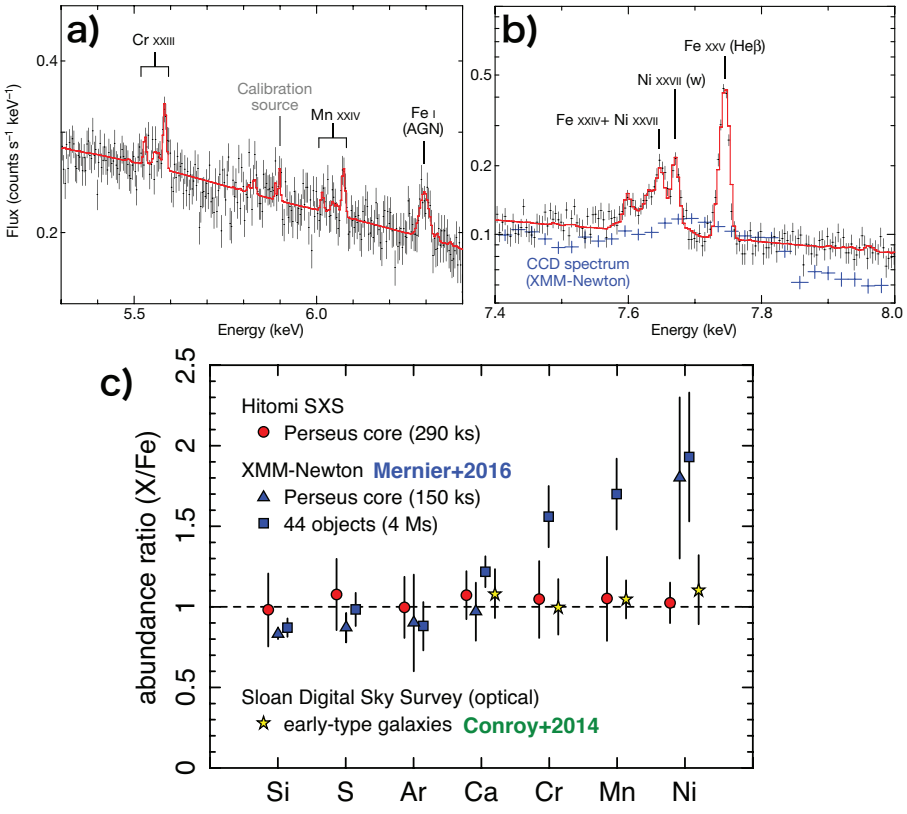

Figure 10: The SXS spectra of a) Cr-Fe energy range, and b) Ni energy range. The weak Kα lines from Cr and Mn are clearly detected. The panel c) shows metal abundances of the Perseus clusters evaluated. The abundances from Ca to Ni are updated. [18]

These observations resolved the Ni-overabundance problem[19], and the elemental abundance of

the Perseus cluster is now revealed to be the same as the solar composition[20]. The iron-peak elements (Cr through Ni) are the products of type Ia SNe. Systematic observations of clusters of galaxies with various redshift and total mass in the future will make it clear chemical evolution of the universe with the iron peak elements as a key.

2.2.5 Testing atomic codes

Now that we have a high resolution spectral data of the thin-thermal hot plasma in the Perseus cluster, we can cross-calibrate so-called the plasma codes [21]. There are three major plasma codes: SPEX[22], ATOMDB[23], and CHIANTI[24]. Among these plasma codes, however, there still remain some 20% difference even in the well-studied iron and nickel emission regions (6.4-7.8 keV). The SXS data on the Perseus cluster are of great use in resolving these differences. Refer to [21] for more detail about the plasma codes cross-calibration.

2.2.6 Possible 3.5 keV line

It has been pointed out that there exists a possible 3.5 keV emission line in an integrated spectrum of 73 clusters of galaxies observed with the *XMM-Newton* MOS [25]. This claim raised a big sensation, because it can be interpreted as a decay of the dark matter candidate "sterile neutrino", and if so, its mass is estimated to be ∼7.1 keV. The SXS, however, does not show any sign of emission line in the region 3.3-3.7 keV[26], as shown in Fig. 11. See [27] a little more detail.

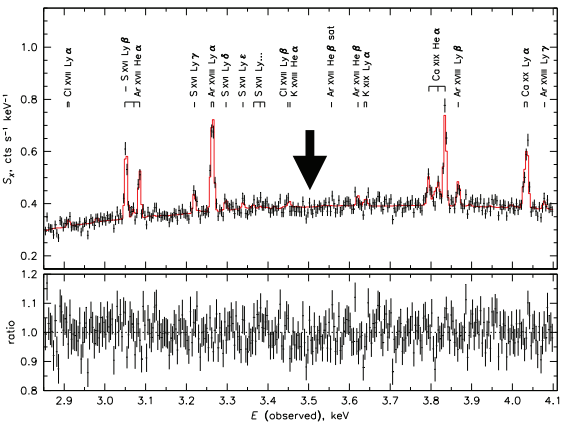

Figure 11: The SXS spectrum of the Perseus cluster in the band 2.85-4.1 keV[26]. The thick arrow indicates the location of the 3.5 keV line.

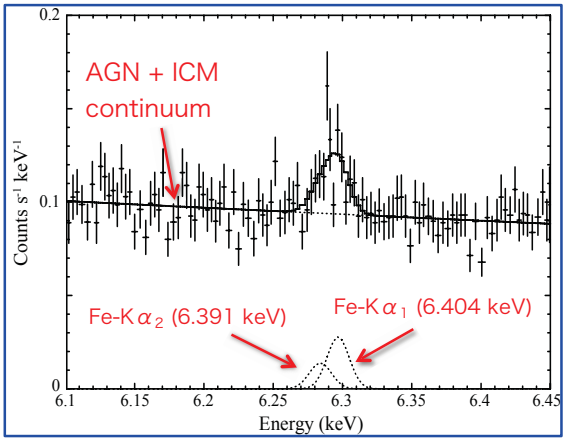

Figure 12: An SXS spectrum of a Kα emission line from neutral iron from the Perseus cluster's cD galaxy NGC 1275 [28].

2.2.7 Fe Kα line from the cD galaxy NGC 1275

The origin of the narrow iron Kα line (6.40 keV) from an AGN has long been a matter of debate for a long time. The SXS high resolution spectroscopy showed its potential power to resolve this issue also in this field. Figure 12 shows the SXS spectrum of NGC 1275, the cD galaxy of the Perseus cluster, in the Fe Kα band 6.1-6.45 keV. The line is weak with an equivalent width of only ∼20 eV. Nevertheless, the SXS successfully detected the line at a confidence level of 5.4σ, and even measured its width to be 500-1,600 km s^{-1} (FWHM) for the first time. Note that a CCD

observation can only measure the width $\geq$10,000 km s^{-1}. The grating spectrometers can do so for the width $\geq$1,000 km s^{-1} but only for bright sources.

The measured velocity width 500-1,600 km s^{-1} is smaller than that of the broad line region (BLR) 2,750 km s^{-1}[29]. The result therefore has rejected the possibility that the neutral iron emission line at 6.4 keV emanates from the BLR, or the accretion disk in the case of NGC 1275. In combination with the image analysis of *Chandra* data, the authors[28] concluded that the line probably originates from a molecular torus, or a circum-nuclear disk, whose velocity is less than several hundred km s^{-1}.

2.3 N132D

N132D is a young and O-rich core-collapsed supernova remnant (SNR) that is brightest among all SNRs in the Large Magellanic Cloud (LMC). Although only 3.7 ksec exposure is retained for the pointing onto N132D due to insufficient calibration of the attitude control system, we have obtained in total 17 and 16 counts in the Heα band of iron and sulphur, whose spectra are shown in Fig. 13 [30]. We remark that, the bulk velocity of iron, measured from the line central energy,

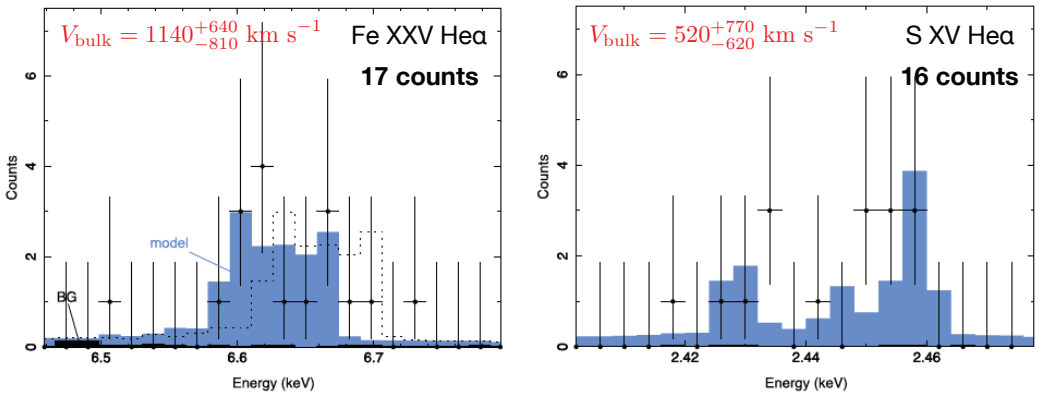

Figure 13: The SXS spectra of N132D in the iron and sulphur Kα line bands. Note that the bulk velocities of iron and sulphur determined from the line central energy are different[30].

$1,140^{+640}_{-810}$ km s^{-1} relative to the LMC's rest frame ($v = +275$ km s^{-1}) is different from that of sulphur, which can be regarded as being at rest in the LMC frame. This result implies that the iron emission originates from the supernova ejecta while sulphur emission comes from ISM material in LMC, and that the ejecta is highly asymmetric. These results demonstrate that even a very small number of counts can directly measure velocities of emission lines from extended objects like SNR, thanks to the high sensitivity of the SXS to the emission lines.

2.4 IGR J16313−4848

IGR J16313−4848 is a high-mass X-ray binary (HMXB) that suffers extremely strong absorption with $N_{\rm H} \simeq 2 \times 10^{24}$ cm^{-2}. Similarity of its X-ray spectrum, including a 6.4 keV iron Kα emission line, suggests this source to be an accreting X-ray pulsar, yet no X-ray pulsation has been detected. Although the SXS exposure time is unfortunately very small, again due to imperfect attitude control like the case of N132D, we still obtained 19 counts in total for an iron Kα 6.4 keV emission line, which is shown in Fig. 14 [31]. The line width corresponds to a velocity of 160^{+300}_{-70}

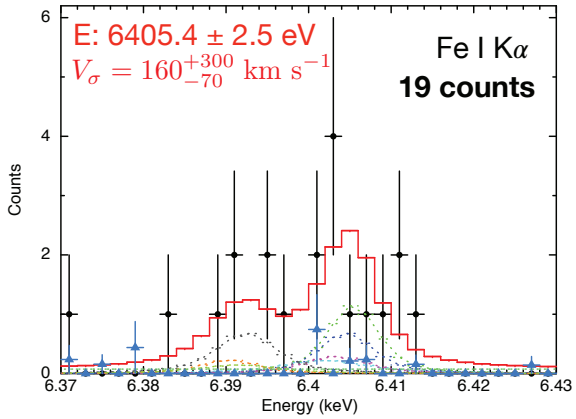

Figure 14: An SXS spectrum of IGR J16313−4848 in the iron Kα band[31].

km s^{-1}, which is the most accurate and smallest width measurement that has ever been achieved. This, together with the iron K-edge energy measurement made with the SXI, results in the ionization state of iron is not more than Fe^{+3} (FeI–IV). From this ionization state, so-called ξ parameter ($\xi = L_{\rm X}/n_{\rm e}\ell^2$) is confined. This ξ parameter and $N_{\rm H}(= n_{\rm e}\ell)$ measured with the SXI and the HXI constrain the electron density and the scale of the fluorescing material to be $n_{\rm e} \geq 3 \times 10^{10}$ cm^{-3} and $\ell \leq 7 \times 10^{13}$ cm. These numbers indicate that the fluorescent iron Kα emission line originates from a cold stellar wind from the massive companion star. This observation provides strong motivation of observing similar HMXB systems with the XRISM mission (§3.1).

2.5 Crab and G21.5−0.9

The Crab nebula has been one of the observation standards for X-ray and γ-ray flux and time, and its origin has been believed to be a core-collapsed supernova (SN). It has, however, some anomalous aspects such as having an uncomfortably small observed ejecta mass 4.6±1.8 $M_\odot$ [32], kinetic energy $< 1 \times 10^{50}$ erg [33], and a maximum velocity of 2,500 km s^{-1} [34]. Nomoto et al. [35] proposed that the Crab nebula was the remnant of an electron-capture supernova, which is caused by electron capture in the O-Ne-Mg core of an intermediate mass progenitor (8-10$M_\odot$). To reinforce or deny this idea, it is important to search the nebula for missing ejecta. Assuming the free expansion velocity of 10^4 km s^{-1}, typical of the core-collapsed SN, extensive search in radio, Hα, and X-ray have been made, but without success. The remaining space is the vicinity of the central pulsar, but very intense radiation from the pulsar from radio to γ-ray precludes us from doing search for the ejecta.

Utilizing an extreme high sensitivity for emission/absorption lines of the SXS, *Hitomi* made a spectroscopic search for a hint of ejecta in the vicinity of the Crab pulsar [36]. Together with reevaluation of the *Chandra* and *XMM-Newton* data, however, *Hitomi* was not able to detect any emission/absorption line from the Crab nebula. The obtained upper limit of the ejecta mass is $<1M_\odot$. This result adds a new piece of support for the electron-capture SN picture.

G21.5−0.9 is one of the composite-type supernova remnants (SNRs) whose emission is dominated by a pulsar wind nebula. A blind search for the emission/absorption line detected a couple of absorption lines at 4.235 keV and 9.296 keV at more than 3σ level [37]. The spectra in these

energy regions are shown in Fig. 15. As can be seen from the spectra, both absorption lines are

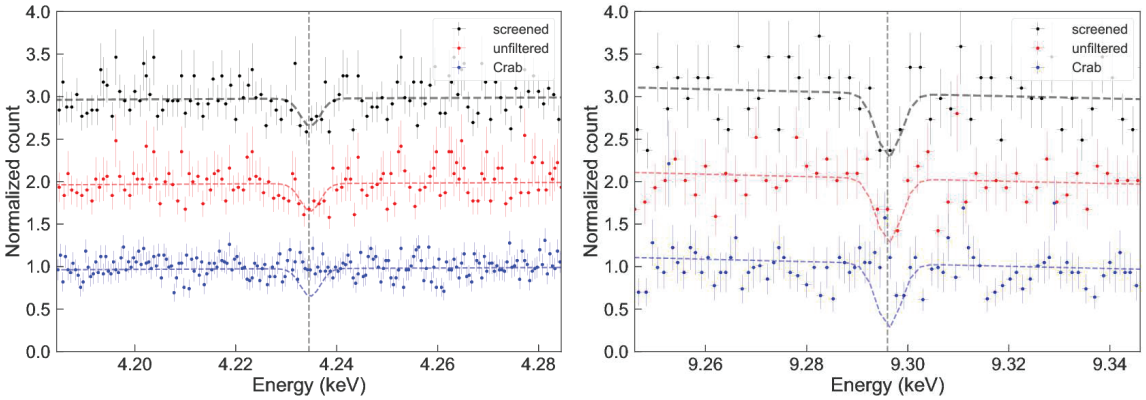

Figure 15: The SXS spectra of G21.5−0.9 in the spectral regions including the absorption lines 4.235 keV and 9.296 keV. The significance levels are bot 3.65σ. Black, red, and blue respectively show the background-unsubtracted spectrum for the screened G21.5−0.9, the unfiltered G21.5−0.9, and the screened Crab data.

detected from G21.5−0.9, whereas no such lines are seen in the Crab spectra. The origin of these lines are still unclear, although they may be due to absorption by neutron star's atmosphere.

3. Future missions

3.1 X-Ray Imaging and Spectroscopy Mission: XRISM

Although *Hitomi* made an extremely high resolution spectroscopy with a non-dispersive detector inorbit for the first time, its life, just one month for the science observations, was too short. It is, however, clearly demonstrated that there is surely a big discovery space to be explored with the X-ray calorimeter. Motivated by this fact, JAXA, in collaboration with NASA, have attempted to retrieve the science with the calorimeter with the recovery mission *XRISM*, which is the abbreviation of *X-Ray Imaging and Spectroscopy Mission*. Figure 16 shows an outlook of *XRISM* in comparison with *Hitomi*. We have a micro-calorimeter system and a CCD camera. Both will be made under completely the same design as that of *Hitomi*. We do not adopt the high-energy instruments HXT/HXI and SGD for reduction of the development cost. We plan to launch *XRISM* with JAXA's H-2A rocket by the end of Japanese fiscal year 2021 (March 2022).

3.2 Focusing On Relativistic universe and Cosmic Evolution: FORCE

FORCE (= *Focusing On Relativistic universe and Cosmic Evolution*) is the next generation hard X-ray mission now being planned in Japan in collaboration with NASA's GSFC. An outlook of *FORCE* is shown in Fig. 17. The science instruments are three identical pairs of an X-ray mirror and a detector that cover an energy range of 1-79 keV with a focal length of 10 m (or two pairs with a focal length of 12 m). It is highly difficult to cover the band 1-79 keV with a single detector, and hence we plan to make a hybrid detector comprising of an SOI (Silicon On Insulator) CMOS, covering the low energy side, and a CdTe, covering the high energy side. The latter is the same as that adopted in *Hitomi*. These sensors are stacked along the X-ray path from the mirror and

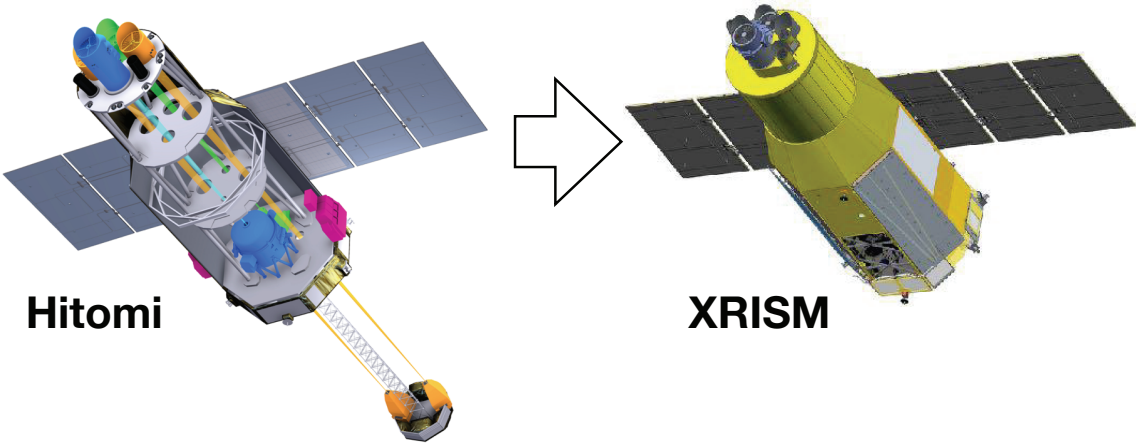

Figure 16: An outlook of *XRIMS* in comparison with that of *Hitomi*.

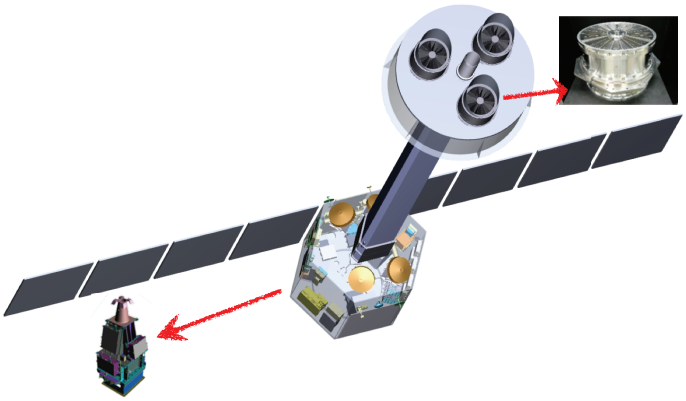

Figure 17: An outlook of the future hard X-ray mission *FORCE*.

embedded in a well of an active shield, aiming at reducing non-X-ray background. The entire detector system is named WHXI (Wide-band Hybrid X-ray Imager).

The X-ray mirror is a light-weight silicon mirror provided by NASA's GSFC. A reflector substrate is lumbered from a silicon ingot, and then polished at high mechanical accuracy. After the polish, Pt/C multilayer is applied onto the concave surface of the substrate to form a reflector sensitive up to 79 keV. The requirement of the angular resolution is 15 arcsec in half-power diameter (HPD), which is better than that of the HXT onboard *Hitomi* (1.7 arcmin [6]) and *NuSTAR* (58 arcsec [38]). A preliminary experiment has verified that the requirement of the HDP is met for a single shell of the reflector.

The HPD of 15 arcsec is comparable with that of *XMM-Newton* below 10 keV. *FORCE* is expected to carry out a high spatial resolution imaging spectroscopy over 10 keV for the first time. With such high spatial resolution, we will be able to carry out a lot of new science. The original main objective of the mission is to complete a census of black holes across cosmic time and mass scale. They include identifying stellar-mass black holes that are currently missing in the Milky Way, revealing the nature intermediate-mass black holes, and surveying accreting supermassive black holes in the universe over the redshift range from 0 to 3. See the document by K. Mori in this

volume for full detail. *FORCE* is now planned to be launched in late 2020's.

4. Summary

Hitomi is the 6th Japanese X-ray astronomy satellite developed in collaboration with US, Europe, and Canada, and was launched on 2016 Feb 17. Unfortunately, however, *Hitomi* was lost on 2016 March 25th, about 1 month from the launch, due to malfunction of the attitude & orbit control system. Nevertheless, *Hitomi* produced many new scientific results even within this short life, owing to extremely high spectral resolution ($E/\Delta E = 1,250$ at 6 keV) of the non-dispersive detector SXS (X-ray micro-calorimeter). The observations of the Perseus cluster produce many scientific results: velocity, resonance scattering, temperature, metal abundance, test of atomic codes, 3.5 keV line, and Fe Kα line from the cD galaxy NGC 1275. Of them, the stringent upper limit of the turbulent pressure, only $<7\%$ of the thermal pressure (§2.2.1) and the metal abundance in ICM consistent to that of the solar vicinity (§2.2.4) are particularly important, and they are published as the two *Nature* papers of *Hitomi* [12, 18]. Power of the high resolution spectroscopy even with small photon counts is demonstrated in N132D and IGR J16318-4848. Emission/absorption line search was performed in Crab and G21.5$-$0.9. A result is obtained to support that the Crab nebula was born from an electron-capture supernova. New absorption line structures are detected from G21.5$-$0.9, although their significance (3-4σ) is not so high.

The *XRISM* project has been on-going to recover the remaining calorimeter science. Following *XRISM*, we started preparing the next generation hard X-ray mission *FORCE* that aims at recovering the lost science of the HXI onboard *Hitomi*, but with much better spatial resolution of 15 arcsec in HPD. They are planned to be launched by the end of March 2022 and late 2020's, respectively.

References

References

[1] T. Takahashi, M. Kokubun, K. Mitsuda, R. L. Kelley, T. Ohashi, F. Aharonian et al., *Hitomi (ASTRO-H) X-ray Astronomy Satellite*, *Journal of Astronomical Telescopes, Instruments, and Systems* **4** (2018) 021402.

[2] Y. Soong, T. Okajima, P. J. Serlemitsos, S. L. Odell, B. D. Ramsey, M. V. Gubarev et al., *ASTRO-H Soft X-ray Telescope (SXT)*, vol. 9144 of *Society of Photo-Optical Instrumentation Engineers (SPIE) Conference Series*, p. 914428. 2014. 10.1117/12.2056804.

[3] R. Iizuka, T. Hayashi, Y. Maeda, M. Ishida, K. Tomikawa, T. Sato et al., *Ground-based x-ray calibration of the Astro-H/Hitomi soft x-ray telescopes*, *Journal of Astronomical Telescopes, Instruments, and Systems* **4** (2018) 011213.

[4] H. Awaki, H. Kunieda, A. Furuzawa, Y. Haba, T. Hayashi, R. Iizuka et al., *ASTRO-H Hard X-ray Telescope (HXT)*, vol. 9144 of *Society of Photo-Optical Instrumentation Engineers (SPIE) Conference Series*, p. 914426. 2014. 10.1117/12.2054633.

[5] H. Mori, T. Miyazawa, H. Awaki, H. Matsumoto, Y. Babazaki, A. Bandai et al., *On-ground calibration of the Hitomi Hard X-ray Telescopes*, *Journal of Astronomical Telescopes, Instruments, and Systems* **4** (2018) 011210.

[6] H. Matsumoto, H. Awaki, M. Ishida, A. Furuzawa, S. Yamauchi, Y. Maeda et al., *Inorbit performance of the Hard X-ray Telescope (HXT) on board the Hitomi (ASTRO-H) satellite*, *Journal of Astronomical Telescopes, Instruments, and Systems* **4** (2018) 011212 [1803.00242].

[7] M. A. Leutenegger, M. Audard, K. R. Boyce, G. V. Brown, M. P. Chiao, M. E. Eckart et al., *In-flight verification of the calibration and performance of the ASTRO-H (Hitomi) Soft X-ray Spectrometer*, *Journal of Astronomical Telescopes, Instruments, and Systems* **4** (2018) 021407.

[8] H. Nakajima, Y. Maeda, H. Uchida, T. Tanaka, H. Tsunemi, K. Hayashida et al., *In-orbit performance of the soft X-ray imaging system aboard Hitomi (ASTRO-H)*, *Publ. Atron. Soc. Japan* **70** (2018) 21 [1709.08829].

[9] K. Nakazawa, G. Sato, M. Kokubun, T. Enoto, Y. Fukazawa, K. Hagino et al., *Hard x-ray imager onboard Hitomi (ASTRO-H)*, *Journal of Astronomical Telescopes, Instruments, and Systems* **4** (2018) 021410.

[10] H. Tajima, S. Watanabe, Y. Fukazawa, R. Bland ford, T. Enoto, A. Goldwurm et al., *Design and performance of Soft Gamma-ray Detector onboard the Hitomi (ASTRO-H) satellite*, *Journal of Astronomical Telescopes, Instruments, and Systems* **4** (2018) 021411.

[11] T. Tamura, Y. Maeda, K. Mitsuda, A. C. Fabian, J. S. Sanders, A. Furuzawa et al., *X-ray Spectroscopy of the Core of the Perseus Cluster with Suzaku: Elemental Abundances in the Intracluster Medium*, *Astrophys. J. Lett.* **705** (2009) L62 [0909.5003].

[12] Hitomi Collaboration, F. Aharonian, H. Akamatsu, F. Akimoto, S. W. Allen, N. Anabuki et al., *The quiescent intracluster medium in the core of the Perseus cluster*, *Nature* **535** (2016) 117 [1607.04487].

[13] Hitomi Collaboration, F. Aharonian, H. Akamatsu, F. Akimoto, S. W. Allen, L. Angelini et al., *Atmospheric gas dynamics in the Perseus cluster observed with Hitomi*, *Publ. Atron. Soc. Japan* **70** (2018) 9 [1711.00240].

[14] E. Churazov, W. Forman, C. Jones and H. Böhringer, *XMM-Newton Observations of the Perseus Cluster. I. The Temperature and Surface Brightness Structure*, *Astrophys. J.* **590** (2003) 225 [astro-ph/0301482].

[15] M. Markevitch and A. Vikhlinin, *Shocks and cold fronts in galaxy clusters*, *Phys. Rep.* **443** (2007) 1 [astro-ph/0701821].

[16] Hitomi Collaboration, F. Aharonian, H. Akamatsu, F. Akimoto, S. W. Allen, L. Angelini et al., *Measurements of resonant scattering in the Perseus Cluster core with Hitomi SXS*, *Publ. Atron. Soc. Japan* **70** (2018) 10 [1710.04648].

[17] Hitomi Collaboration, F. Aharonian, H. Akamatsu, F. Akimoto, S. W. Allen, L. Angelini et al., *Temperature structure in the Perseus cluster core observed with Hitomi*, *Publ. Atron. Soc. Japan* **70** (2018) 11 [1712.06612].

[18] Hitomi Collaboration, F. Aharonian, H. Akamatsu, F. Akimoto, S. W. Allen, L. Angelini et al., *Solar abundance ratios of the iron-peak elements in the Perseus cluster*, *Nature* **551** (2017) 478 [1711.10035].

[19] F. Mernier, J. de Plaa, C. Pinto, J. S. Kaastra, P. Kosec, Y. Y. Zhang et al., *Origin of central abundances in the hot intra-cluster medium. I. Individual and average abundance ratios from XMM-Newton EPIC*, *Astron. Astrophys.* **592** (2016) A157 [1606.01165].

[20] C. Conroy, G. J. Graves and P. G. van Dokkum, *Early-type Galaxy Archeology: Ages, Abundance Ratios, and Effective Temperatures from Full-spectrum Fitting*, *Astrophys. J.* **780** (2014) 33 [1303.6629].

[21] Hitomi Collaboration, F. Aharonian, H. Akamatsu, F. Akimoto, S. W. Allen, L. Angelini et al., *Atomic data and spectral modeling constraints from high-resolution X-ray observations of the Perseus cluster with Hitomi*, *Publ. Atron. Soc. Japan* **70** (2018) 12 [1712.05407].

[22] J. S. Kaastra, R. Mewe and H. Nieuwenhuijzen, *SPEX: a new code for spectral analysis of X & UV spectra.*, in *UV and X-ray Spectroscopy of Astrophysical and Laboratory Plasmas*, pp. 411–414, Jan, 1996.

[23] A. R. Foster, L. Ji, R. K. Smith and N. S. Brickhouse, *Updated Atomic Data and Calculations for X-Ray Spectroscopy*, *Astrophys. J.* **756** (2012) 128 [1207.0576].

[24] G. Del Zanna, K. P. Dere, P. R. Young, E. Landi and H. E. Mason, *CHIANTI - An atomic database for emission lines. Version 8*, *Astron. Astrophys.* **582** (2015) A56 [1508.07631].

[25] E. Bulbul, M. Markevitch, A. Foster, R. a. K. Smith, M. Loewenstein and S. W. Randall, *Detection of an Unidentified Emission Line in the Stacked X-Ray Spectrum of Galaxy Clusters*, *Astrophys. J.* **789** (2014) 13 [1402.2301].

[26] F. A. Aharonian, H. Akamatsu, F. Akimoto, S. W. Allen, L. Angelini, K. A. Arnaud et al., *Hitomi Constraints on the 3.5 keV Line in the Perseus Galaxy Cluster*, *Astrophys. J. Lett.* **837** (2017) L15 [1607.07420].

[27] M. Ishida and Hitomi Collaboration, *Highlights from the X-ray Astronomy Satellite Hitomi (ASTRO-H)*, in *XII Multifrequency Behaviour of High Energy Cosmic Sources Workshop (MULTIF2017)*, p. 46, Jun, 2017.

[28] Hitomi Collaboration, F. Aharonian, H. Akamatsu, F. Akimoto, S. W. Allen, L. Angelini et al., *Hitomi observation of radio galaxy NGC 1275: The first X-ray microcalorimeter spectroscopy of Fe-Kα line emission from an active galactic nucleus*, *Publ. Atron. Soc. Japan* **70** (2018) 13 [1711.06289].

[29] L. C. Ho, A. V. Filippenko and W. L. W. Sargent, *A Search for "Dwarf" Seyfert Nuclei. III. Spectroscopic Parameters and Properties of the Host Galaxies*, *Astrophys. J. Suppl.* **112** (1997) 315 [astro-ph/9704107].

[30] Hitomi Collaboration, F. Aharonian, H. Akamatsu, F. Akimoto, S. W. Allen, L. Angelini et al., *Hitomi observations of the LMC SNR N 132 D: Highly redshifted X-ray emission from iron ejecta*, *Publ. Atron. Soc. Japan* **70** (2018) 16 [1712.02365].

[31] Hitomi Collaboration, F. Aharonian, H. Akamatsu, F. Akimoto, S. W. Allen, L. Angelini et al., *Glimpse of the highly obscured HMXB IGR J16318-4848 with Hitomi*, *Publ. Atron. Soc. Japan* **70** (2018) 17 [1711.07727].

[32] R. A. Fesen, J. M. Shull and A. P. Hurford, *An Optical Study of the Circumstellar Environment Around the Crab Nebula*, *Astron. J.* **113** (1997) 354.

[33] K. Davidson and R. A. Fesen, *Recent developments concerning the Crab Nebula.*, *Annual Rev. Astron. Astrophys.* **23** (1985) 119.

[34] J. Sollerman, P. Lundqvist, D. Lindler, R. A. Chevalier, C. Fransson, T. R. Gull et al., *Observations of the Crab Nebula and Its Pulsar in the Far-Ultraviolet and in the Optical*, *Astrophys. J.* **537** (2000) 861 [astro-ph/0002374].

[35] K. Nomoto, W. M. Sparks, R. A. Fesen, T. R. Gull, S. Miyaji and D. Sugimoto, *The Crab Nebula's progenitor*, *Nature* **299** (1982) 803.

[36] Hitomi Collaboration, F. Aharonian, H. Akamatsu, F. Akimoto, S. W. Allen, L. Angelini et al., *Search for thermal X-ray features from the Crab nebula with the Hitomi soft X-ray spectrometer*, *Publ. Atron. Soc. Japan* **70** (2018) 14 [1707.00054].

[37] Hitomi Collaboration, F. Aharonian, H. Akamatsu, F. Akimoto, S. W. Allen, L. Angelini et al., *Hitomi X-ray observation of the pulsar wind nebula G21.5-0.9*, *Publ. Atron. Soc. Japan* **70** (2018) 38 [1802.05068].

[38] F. A. Harrison, W. W. Craig, F. E. Christensen, C. J. Hailey, W. W. Zhang, S. E. Boggs et al., *The Nuclear Spectroscopic Telescope Array (NuSTAR) High-energy X-Ray Mission*, *Astrophys. J.* **770** (2013) 103 [1301.7307].

DISCUSSION

JAMES HOWARTH BEAL: When will the *FORCE* mission approved ?

MANABU ISHIDA: We expect that the approval of *FORCE* by JAXA as a project is July 2022.